Human Movement Science 61 (2018) 52–62

Contents lists available at ScienceDirect

Human Movement Science

journal homepage: www.elsevier.com/locate/humov

Full Length Article

Investigation of isochrony phenomenon based on the computational theory of human arm trajectory planning

Hiroshi Yokoyama*, Hiashi Saito, Rie Kurai, Isao Nambu, Yasuhiro Wada

Graduate School of Engineering, Nagaoka University of Technology, 1603-1 Kamitomioka, Nagaoka, Niigata 940-2188, Japan

ARTICLE INFO

Keywords:
Human arm movement
Trajectory planning
Human isochrony
Isochrony phenomenon
Minimum commanded torque change criterion
Via-point movement

ABSTRACT

The isochrony principle is a well-known phenomenon whereby the speed of human arm movement is regulated to increase as its trajectory distance increases. However, the relationship between the trajectory planning and the isochrony phenomenon has never been sufficiently explained. One computational study derived the algorithm for estimating the optimal movement segmentation and its duration based on the framework of the minimum commanded torque change criterion. By extending this finding, we can consider the hypothesis that the human arm trajectory is generated based on the minimum commanded torque change criterion to ensure that the duration average of the commanded torque changes (DCTCs) are equivalent between certain movement segmentations, rather than to satisfy the isochrony phenomenon. To test this hypothesis, we measured the behavioral performance of hand movement tasks in which subjects write eight-shaped and double-elliptical-shaped trajectories including two similar shaped arcs of different sizes (hereafter called large and small loops). Our results indicate that the human arm movement is planned in such a manner that the DCTCs for the large and small loops are equivalent during writing of the double-elliptical-shaped trajectories regardless of the arc size. A similar tendency was also observed for the data during the eight-shaped movements, although the ratio of the DCTCs slightly changed depending on the arc size conditions. Thus, our study provides experimental evidence that the isochrony phenomenon is ensured through the computational process of trajectory planning.

1. Introduction

The isochrony principle (Viviani & McCollum, 1983; Viviani & Flash, 1995; Sartori, Camperio-Ciani, Bulgheroni, & Castiello, 2013; Flash, Meirovitch, & Barliya, 2013; Viviani & Terzuolo, 1982) is known as a specific phenomenon of motor control, whereby the speed of hand reaching movement is regulated to increase as its trajectory distance increases. For instance, when a subject draws the eight-shaped symbol shown in Fig. 1 by hand, the time required to write both arcs that form this symbol is approximately equivalent, and is independent of the difference in perimeter distance between each arc. Early studies of this phenomenon found experimental evidence that the movement speed increases relative to the movement size to ensure a stable movement time (Viviani & McCollum, 1983; Viviani & Flash, 1995). The latest studies on the isochrony principle (Flash et al., 2013) considered the computational relationship between changes in the movement speed and changes in the movement size to satisfy this principle. However, these studies did not include a detailed investigation of the computational process between trajectory planning and the isochrony principle, focusing instead on the geometrical relationship between movement speed and movement size (Flash et al., 2013). To

* Corresponding author.
E-mail address: h_yokoyama@stn.nagaokaut.ac.jp (H. Yokoyama).

https://doi.org/10.1016/j.humov.2018.07.001
Received 18 January 2018; Received in revised form 30 June 2018; Accepted 2 July 2018
Available online 14 July 2018

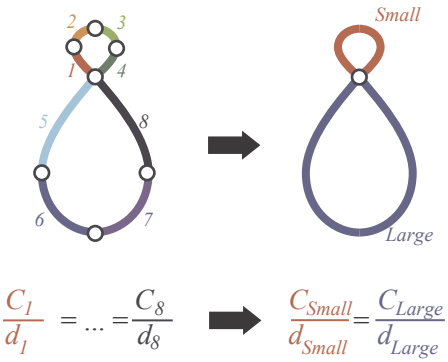

Fig. 1. Schematic view of our hypothesis. Considering that the movement time is adjusted to satisfy the constant DCTC for each via-point based on Eq. (5), this suggests that the DCTCs for the upper and lower arcs are modified to ensure that $C_{Large}/d_{Large} = C_{Small}/d_{Small}$.

account for the isochrony phenomenon in the motor control of human arm movement, there is a need to identify how the movement trajectory is generated while optimizing the movement time to ensure the isochrony phenomenon in association with the computational model of trajectory planning.

Various trajectory planning criteria have been proposed, such as the minimum jerk criterion (Flash & Hogan, 1985; Edelman & Flash, 1987; Kyriakopoulos & Saridis, 1988), minimum torque change criterion (Uno, Kawato, & Suzuki, 1989; Kawato, Maeda, Uno, & Suzuki, 1990), and the minimum muscle tension change criterion (Dornay, Kawato, & Suzuki, 1996; Kudo, Choi, Kagawa, & Uno, 2016). In general, when we apply these models to generate a simulated optimal trajectory of human hand-drawing, geometrical information about the start and end points is required as a boundary condition. Further, in the case of generating a complex trajectory, such models assume that the movement trajectory must pass from start to end through some specified points (so-called via-points) (Edelman & Flash, 1987); naturally, information of both the location and transit time of each via-point is also required for the boundary condition. Therefore, these conventional models cannot solve the issue of how the human brain plans an optimized trajectory and movement time in parallel to satisfy the isochrony phenomenon.

Certain computational studies on the trajectory planning for human arm movement (Wada & Kawato, 1993; Nakano et al., 1999; Wada, Kaneko, Nakano, Osu, & Kawato, 2001; Wada & Kawato, 2004) could be considered as a relevant solution to the above issue. On the basis of the framework of the minimum commanded torque change criterion, these authors (Wada & Kawato, 1993; Nakano et al., 1999; Wada et al., 2001; Wada & Kawato, 2004) provided an optimization algorithm for trajectory planning, which can coincidentally satisfy the following two problems: (1) estimation of some via-points to draw the optimal trajectory, and (2) derivation of the updated rule of the transit time of arm movement between each via-point to ensure a constant commanded torque change. Therefore, the proposed algorithm could estimate both the optimal via-point and via-to-via movement time during complex hand movement tasks based on the framework of the minimum commanded torque change criterion. In addition, this algorithm can generate a simulated trajectory so that the average duration of the commanded torque change (so-called DCTC) is equivalent in each via-to-via movement interval (these intervals are virtually partitioned by the via-points) (Wada & Kawato, 2004). By extending the above computational relationship to the DCTC condition and movement interval with the commanded torque change model, two previous studies (Saito, Tsubone, & Wada, 2006; Saito & Wada, 2006) suggested the possibility that the isochrony principle can be explained by computational theory based on the minimum commanded torque change model. Thus, the above mentioned algorithm (Wada & Kawato, 1993; Nakano et al., 1999; Wada et al., 2001; Wada & Kawato, 2004) could extend as the fundamental principle to understand how the isochrony phenomenon is ensured during human arm movement. However, experimental evidence is lacking to support this possible assumption.

In this paper, we address the issue of whether the isochrony principle can be explained by computational theory based on the minimum commanded torque change model (Wada & Kawato, 2004; Saito et al., 2006; Saito & Wada, 2006). We then hypothesize that the trajectory of human arm movement generates to satisfy the constant DCTC between large and small loops, rather than to ensure constant movement times (Wada & Kawato, 2004; Saito et al., 2006; Saito & Wada, 2006). To test this hypothesis with experimental data, we conduct two different hand reaching tasks (eight-shaped trajectory and double-elliptical-shaped trajectory) that were applied in previous isochrony studies (Viviani & McCollum, 1983; Flash et al., 2013). In the analysis, we first estimated the via-points and the time using the above-mentioned algorithm (Wada & Kawato, 2004) and separated the movement segments (i.e. different size of loops). Then we evaluated the DCTCs among different movement intervals to consider how the joint-torque changes are controlled during the hand movement tasks.

2. Relationship between via-point time optimization algorithm and isochrony phenomenon

The minimum commanded torque change criterion (Nakano et al., 1999; Wada et al., 2001) is defined as the following equation:

$$C_\tau = \int_0^T \sum_{k=1}^{K} \left(\frac{d\tau^k}{dt}\right)^2 dt = \sum_i C_i = \sum_i \int_{t_{i-1}}^{t_i} \sum_{k=1}^{K} \left(\frac{d\tau_t^k}{dt}\right)^2 dt \quad (1)$$

where C_τ is the objective function of the criterion, T indicates the movement time, K indicates the total number of joint, τ^k indicates the k-th joint torque (k = 1: *shoulder*;k = 2: *elbow*), C_i is the objective function for the i-th via-point (i = 1, 2, ...,n), and t_i is also the movement time of the i-th via-point. Thus, this criterion optimizes the hand movement trajectory so that the total torque change in each via-to-via movement interval is minimized. On the basis of the framework of the minimum commanded torque change criterion, these authors (Nakano et al., 1999; Wada et al., 2001; Wada & Kawato, 2004) provided an optimization algorithm for trajectory planning, which can coincidentally satisfy the following two problems: (1) estimation of some via-points to draw the optimal trajectory, and (2) derivation of the updated rule of the transit time of arm movement between each via-point to ensure a constant commanded torque change. Therefore, this algorithm could estimate both the optimal via-point and via-to-via movement time during complex hand movement tasks based on the framework of the minimum commanded torque change criterion. Moreover, in this algorithm, the commanded torque is adjusted to ensure the following relationship:

$$DCTC_i^{via} = \frac{1}{t_i - t_{i-1}} \int_{t_{i-1}}^{t_i} \sum_{k=1}^{K} \left(\frac{d\tau_k}{dt}\right)^2 dt = \frac{C_i}{d_i} \quad (2)$$

$$\frac{C_1}{d_1} = \cdots = \frac{C_n}{d_n} \quad (3)$$

where $DCTC_i^{via}$ ($=C_i/d_i$) is the duration average of the commanded-torques with via-point i, d_i is the movement time from the $i-1$-th to the i-th via-point, and C_i is the objective function of the criterion with via-point i. Thus, the algorithm adjusts not only the trajectory, but also the movement time, while ensuring a constant DCTC in each via-point interval. Considering the DCTC relationship in each via-point interval, as shown in Eq. (3), previous studies (Saito et al., 2006; Saito & Wada, 2006) have explained the possibility that the DCTC is equalized to satisfy Eq. (3) and Eq. (4), as shown in Fig. 1:

$$DCTC_{Small} = \frac{C_{Small}}{d_{Small}} = \frac{C_{Large}}{d_{Large}} = DCTC_{Large} \quad (4)$$

where '*small*' and '*large*' indicate the small and large segmentations (see the red and blue segmentations in Fig. 1). The mathematical proof of Eq. (4) is simple. If the index p indicating the point separating the large and small loops exists, then the DCTC relationship between the large and small loops can be considered as follows:

$$\frac{C_1}{d_1} = \frac{C_2}{d_2} = \ldots = \frac{C_{p-1}}{d_{p-1}} = \frac{C_p}{d_p} = \ldots = \frac{C_n}{d_n} \quad (5)$$

Small loop.

$$\begin{aligned} C_1 &= \alpha C_2, & d_1 &= \alpha d_2 \\ C_1 &= \beta C_3, & d_1 &= \beta d_3 \\ &\vdots \\ C_1 &= x C_{p-1}, & d_1 &= x d_{p-1} \end{aligned} \quad (6)$$

Large loop.

$$\begin{aligned} C_p &= \gamma C_{p+1}, & d_s &= \gamma d_{p+1} \\ C_p &= \zeta C_{p+2}, & d_s &= \zeta d_{p+2} \\ &\vdots \\ C_p &= y C_n, & d_s &= y d_n \end{aligned} \quad (7)$$

Note that α, β, ...,x and γ, ζ, ...,y indicate positive constant parameters. Considering Eqs. (5)–(7), C_1/d_1 and C_p/d_p can be rewritten as:

$$\frac{C_1 + C_2 + \cdots + C_{p-1}}{d_1 + d_2 + \cdots + d_{p-1}} = \frac{(1 + 1/\alpha + 1/\beta + \cdots + 1/x)C_1}{(1 + 1/\alpha + 1/\beta + \cdots + 1/x)d_1} = \frac{C_1}{d_1} \quad (8)$$

$$\frac{C_p + C_{p+1} + \cdots + C_n}{d_p + d_{p+1} + \cdots + d_n} = \frac{(1 + 1/\gamma + 1/\zeta + \cdots + 1/y)C_p}{(1 + 1/\gamma + 1/\zeta + \cdots + 1/y)d_p} = \frac{C_p}{d_p} \quad (9)$$

$$\begin{aligned} &\frac{C_1}{d_1} = \frac{C_p}{d_p} \\ &\frac{C_1 + C_2 + \cdots + C_{p-1}}{d_1 + d_2 + \cdots + d_{p-1}} = \frac{C_p + C_{p+1} + \cdots + C_n}{d_p + d_{p+1} + \cdots + d_n} \\ &\therefore \quad \frac{C_{Small}}{d_{Small}} = \frac{C_{Large}}{d_{Large}} \end{aligned} \quad (10)$$

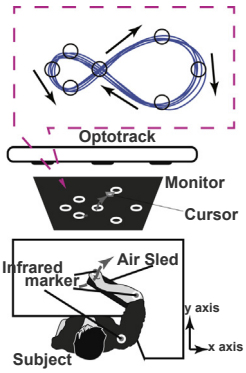

Fig. 2. Experimental environment. Subjects sat on a chair placed in front of a monitor. During the tasks, hand movements were measured by the 3-dimensional motion capture system, and the current position of the hand was provided as visual feedback on the monitor.

Considering the above computational relationship, two previous studies (Saito et al., 2006; Saito & Wada, 2006) suggested a possible hypothesis where the isochrony principle can be explained by computational theory based on the minimum commanded torque change model. To test this hypothesis, we revealed whether the relationship with the DCTCs among different movement intervals follows the above-mentioned computational theory (see Fig. 1) with experimental data.

3. Materials and methods

3.1. Subject

Fifteen healthy right-handed males (mean age: 22 years old) participated in the experiments. This study was approved by the Ethics Committee of Nagaoka University of Technology and all procedures were performed in accordance with the Declaration of Helsinki (version 2008). All subjects provided written informed consent before the experiments.

3.2. Experimental environment

The experimental environment is illustrated in Fig. 2. The subjects sat on a chair placed in front of a monitor, and their wrists were supported by a brace with an air sled to reduce the influence of friction. Moreover, infrared markers were positioned on the hand, elbow, and shoulder of each subject to measure the arm movement trajectory while performing the task. The movement trajectories in each marker were measured by a 3-dimensional motion capture system (Optotrak Certus, Northern Digital Inc., Waterloo, Canada; sampling frequency: 200 Hz).

3.3. Task procedure

Two trajectory patterns were applied for the cyclic arm movement task, as shown in Fig. 3. The first was an eight-shaped trajectory (the so-called figure- eight, Fig. 3A), which has three different variations of perimeter ratio between the left and right loops (hereafter called the large and small loops). The second pattern was a double-elliptical trajectory (the so-called double-ellipse, Fig. 3B), which has two different variations of perimeter ratio between the large and small loops. The movement distance between the large and small loops varies. In total, five different trajectory patterns (three figure-eight and two double-ellipse patterns) were designed to determine the effect of this difference on the isochrony phenomenon.

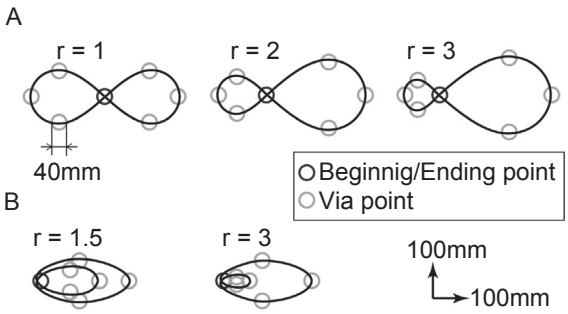

Fig. 3. Template of trajectory shapes. (A) The figure-eight task has three different variations of the perimeter ratio between left and right loops (r = 1.0, 2.0, 3.0). (B) The double-ellipse task has two different variations of the perimeter ratio between the loops (r = 1.5, 3.0).

The following describes how the tasks were performed for each pattern (Fig. 3). First, target markers and a cursor were shown on the monitor, and the subjects were instructed to move the cursor, which was provided visual feedback as to the current position of the hand, to the start position (Fig. 3). Upon hearing a starting beep, the subjects were then directed to move the cursor from start point to end point in the order of large to small loops for five cycles. They were required to finish this reaching task within 10 s of the starting beep. A second beep sound 10 s after the starting beep informed the subjects that the rest interval had started; this interval lasted 5 s, after which the next task commenced. During the rest intervals, the subjects were instructed to keep their hand in a relaxed state at the start point position. For each trajectory shape, this procedure was executed 30 times over three sessions (30 trials = 10 trials × 3 sessions).

3.4. Analysis

3.4.1. Preprocessing

The trajectory data were filtered using a sixth-order Butterworth filter with a cutoff frequency of 10 Hz. The threshold to determine the start and end points of hand movement was set to 5% of the maximum tangential velocity. This threshold was evaluated for each trial. Then, the time-intervals for which the tangential velocity was greater than this threshold were analyzed as the actual movement intervals. Further, the first and last cycle of the five cycles in each trial were excluded from the analysis because these cycles contained unstable actions associated with the start or termination of movement.

3.4.2. Inverse dynamics model

In this study, to estimate the movement via-point and the movement time in each via-point based on the minimum commanded-torque change criterion, the joint-torque had to be calculated during hand movement. Therefore, we evaluated the joint-torque (τ_1, τ_2) using the inverse dynamics model, given by the following equation:

$$\begin{aligned}\tau_1 =& (I_1 + I_2 + 2M_2L_1S_2\cos(\theta_2) + M_2(L_1)^2)\ddot{\theta}_1 \\ &+ (I_2 + M_2L_1S_2\cos(\theta_2))\ddot{\theta}_2 \\ &- (M_2L_1S_2(2\dot{\theta}_1 + \dot{\theta}_2))\dot{\theta}_2\sin(\theta_2) + B_{11}\dot{\theta}_1 + B_{12}\dot{\theta}_2 \\ \tau_2 =& (I_2 + M_2L_1S_2\cos(\theta_2))\ddot{\theta}_1 + I_2\ddot{\theta}_2 \\ &+ M_2L_1S_2(\dot{\theta}_1)^2\sin(\theta_2) + B_{21}\dot{\theta}_1 + B_{22}\dot{\theta}_2 \end{aligned} \quad (11)$$

where θ_i, $\dot{\theta}_i$, and $\ddot{\theta}_i$ represent the position, velocity, and acceleration of each joint, respectively. M_i, L_i, S_i, I_i and B_{ij} indicate the mass, joint length, distance from the mass center to the joint, rotary inertia of link i around the joint, and the coefficients of viscosity, respectively. Joints 1 and 2 correspond to the shoulder and elbow, respectively. For each subject, M_i, S_i, and I_i were estimated by the link length L_i based on the previous study (Nakano et al., 1999). Moreover, the coefficients of viscosity B_{ij} were estimated using the following equation, proposed by Gomi and Osu (1998).

$$[B_{11}, B_{12}(=B_{21}), B_{22}] = [-0.63 + 0.095\tau_1^{ma}, 0.175 + 0.0375\tau_2^{ma}, 0.760 + 0.185\tau_2^{ma}], \quad \text{Nm/(rad/s)} \quad (12)$$

where τ_1^{ma} and τ_2^{ma} indicate the mean absolute torques for each joint during movement, calculated using Eq. (11) with zero viscosity. The averaged value for each estimated dynamic parameter is shown in Table 1.

3.4.3. Via-point time estimation and loop separation

In the analysis, the measured hand movement trajectories were separated as small and large loops based on the movement via-points, which were estimated by the above-mentioned via-point time optimization algorithm based on the minimum commanded torque changes criterion Wada and Kawato (2004). This algorithm estimates both the movement via-point and via-point time by way of the following 3 steps (see the text in Wada & Kawato (2004) for the details).

Step 1 Predict the trajectories using the Forward Inverse Relaxation Model (Wada & Kawato, 1993) according to a set of initial via-

Table 1
List of the estimated dynamic parameters. Each element indicates the group average value of the dynamic parameters with inter-subject standard deviation (mean ± SD). The methods of Gomi and Osu (1998) and Nakano et al. (1999) were applied to this estimation. L_i, M_i, S_i, I_i, B_{ij} represent the length, mass, distance from the mass center to the joint, the rotary inertia of link i around the joint, and the coefficients of viscosity, respectively. See the text for more detail.

	Link 1	Link 2
L_i [m]	0.2725 ± 0.0236	0.3262 ± 0.0200
M_i [kg]	1.3456 ± 0.1284	1.0576 ± 0.0592
S_i [m]	0.1017 ± 0.0097	0.1596 ± 0.0089
I_i [kg m^2]	0.0220 ± 0.0065	0.0406 ± 0.0068
B_{11}, B_{22} [kg m^2/s]	0.7631 ± 0.0607	0.8440 ± 0.0396
B_{12}, B_{21} [kg m^2/s]	0.1920 ± 0.0080	0.1920 ± 0.0080

point times.
Step 2 Update the via-point time to minimize the commanded torque change using the steepest descent method.
Step 3 Correct the movement time in each via-point so that the total movement time of the predicted trajectory satisfies the entire movement duration of the predicted trajectory.

Using the above algorithm, the movement via-point and the movement time in each via-point were estimated in parallel to satisfy the minimum commanded-torque change criterion. The following description of all analyses excluded the trial in which the via-point estimation, based on the above-mentioned algorithm, did not converge due to measured noise or irregular behavior during reaching tasks.

Next, the movement trajectory was separated into small and large loops according to the estimated via-points. The reference points used to separate the loops were selected within the estimated via-points, located as the nearest movement point relative to the start/end point, with cycle-by-cycle in each trial. These procedures were applied for each task for all participants and the estimated movement intervals for the small and large loops were employed to evaluate the movement time r_d and DCTC ratio r_τ to ensure application of the isochrony principle, as described later.

3.4.4. Movement time ratio

We then evaluated the movement time ratio r_d to test whether the hand movement is performed to ensure the isochrony principle. The ratio of movement times between large and small loops was calculated as:

$$r_d = \frac{1}{3}\sum_{k=2}^{4}\frac{t_{L,k}}{t_{S,k}} \tag{13}$$

where $t_{L,k}$ and $t_{S,k}$ denote the movement times for large and small loops with the number of movement cycles k (=2, 3, 4). As described above, the first and last cycles of the five cycles in each trial and the trial containing the via-point estimation error were excluded from the analysis.

3.4.5. DCTC ratio

We evaluated the DCTC ratio r_τ to test whether the hand movement is performed to ensure the constant commanded-torque changes between loops. The DCTC value in each loop was calculated based on Eq. (2) using the computed values of the commanded torques (τ_1, τ_2). The ratio of DCTC between large and small loops was calculated as:

$$r_\tau = \frac{1}{3}\sum_{k=2}^{4}\frac{DCTC_{L,k}}{DCTC_{S,k}} \tag{14}$$

where $DCTC_{L,k}$ and $DCTC_{S,k}$ denote the DCTC of large and small loops with the number of movement cycles k (=2, 3, 4). The same procedure for the movement time ratio was used to exclude errors and unstable data/trials.

3.4.6. Two sample t-test and two one-sided t-test (TOST)

In order to validate which of the two ratios r_d and r_τ reflects the constancy during hand movement, we applied two types of t-test, two sample t-tests and two one-sided t-tests (TOSTs) (Lakens, 2017).

First, applying the two sample t-tests, we tested whether each ratio r_d and r_τ shows a statistically significant difference depending on the condition of the perimeter ratio r or not. The significance level of differences iwas evaluated based on the following equations:

$$t_{diff} = \frac{\overline{M}_1 - \overline{M}_2}{\sigma\sqrt{\frac{1}{n_1}+\frac{1}{n_2}}},$$
$$\sigma = \sqrt{\frac{(n_1-1)SD_1^2 + (n_2-1)SD_2^2}{n_1+n_2-2}} \tag{15}$$

where n_1 and n_2 indicate the number of each sample, $\overline{M}_1$ and $\overline{M}_2$ indicate the mean of each sample, and σ indicates the pooled standard deviation between the two samples.

Next, applying TOSTs, we tested the equivalence of each ratio under different conditions of the perimeter ratio r. In this statistical test, if a $(1-2\alpha) \times 100\%$ confidence interval for the difference in r_τ, under different conditions of r, is contained within the interval $[-\delta, +\delta]$, then equivalence was established at the significance level (Lakens, 2017). In particular, the TOSTs validated whether the differences between the two samples were sufficiently larger than the lower boundary $-\delta$ (right sided test) or sufficiently smaller than the upper boundary $+\delta$ (left sided test). The significance level of equivalence in the TOSTs was evaluated based on the following equations (Lakens, 2017):

$$t_L = \frac{\overline{M}_1 - \overline{M}_2 - (-\delta)}{\sigma\sqrt{\frac{1}{n_1}+\frac{1}{n_2}}}, \quad and \quad t_U = \frac{\overline{M}_1 - \overline{M}_2 - (+\delta)}{\sigma\sqrt{\frac{1}{n_1}+\frac{1}{n_2}}}$$
$$\sigma = \sqrt{\frac{(n_1-1)SD_1^2 + (n_2-1)SD_2^2}{n_1+n_2-2}} \tag{16}$$

Note that the equivalence boundary $[-\delta, +\delta]$ is set as $\delta = 0.3$ in this study.

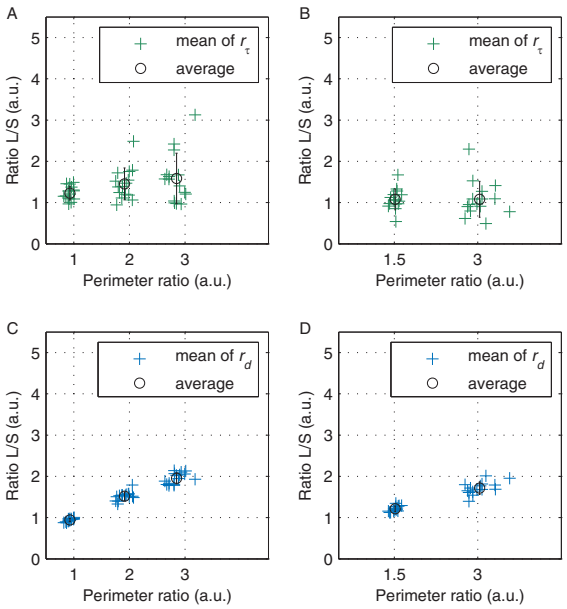

Fig. 4. Group-averaged results of the DCTC ratio r_τ and the movement duration ratio r_d. Results of r_τ for (A) the figure-eight task and (B) the double-ellipse task. Results of r_d for (C) the figure-eight task and (D) the double-ellipse task. The circular symbols indicate group-averaged data over all subjects for r_τ and r_d. Crosses (+) denote trial-averaged data in each subject. Error bars show the standard deviation (SD) for r_τ and r_d across subjects.

Using these two types of t-test, each r_d and r_τ was directly compared under different conditions of the perimeter ratio r for each trajectory shape. Moreover, in these tests, the pair of r_* ($*$ indicates the torque changes τ or duration d), under different conditions of the perimeter ratio r, were directly compared for each trajectory shape (figure-eight: $r_{*|r=1.0}$ vs $r_{*|r=2.0}$, $r_{*|r=1.0}$ vs $r_{*|r=3.0}$, $r_{*|r=2.0}$ vs $r_{*|r=3.0}$; double-ellipse task: $r_{*|r=1.5}$ vs $r_{*|r=3.0}$). Note that we used trial-averaged data for each subject (i.e. within-subject average) as a sample for the ratio r_*. Further, the values of p, given in the results of the figure-eight task, were corrected with the effect of multiple comparison by the false discovery rate method (FDR) (Benjamini & Hochberg, 1995).

4. Results

4.1. Movement duration ratio and DCTC ratio

We first calculated the movement time ratio r_d and DCTC ratio r_τ between the loops in each trajectory shape to evaluate how the movement time and the joint-torque changes are affected by the difference in the movement perimeter between the loops. Fig. 4 shows the results for both r_d and r_τ (Fig. 4A: r_τ in the figure-eight task, B: r_τ in the double-ellipse task, C: r_d in the figure-eight task, D: r_d in the double-ellipse task). The scatter plots in this figure show the trial-averaged value for each subject. While r_d indicates an increase relative to the increasing movement distance in both trajectory shapes (r_d = around 1.0–2.0; Fig. 4C, D), r_τ tends to remain constant between large and small loops, regardless of differences in the movement distance (Fig. 4A, B). The group-averaged r_τ was around 1.2–1.6 for the figure-eight task and around 1.0–1.1 for the double-ellipse task.

4.2. Statistical test in each ratio

To test whether r_τ and r_d are constant regardless of the perimeter ratio r, we applied two types of t-test (two sample t-tests and TOSTs).

We first show the results of these statistical tests for r_τ in Table 2 and Fig. 5. Table 2 presents the statistical details of both the two sample t-tests and the TOSTs for r_τ. As shown by the results of the significant difference test with two sample t-tests, both the figure-eight and double-ellipse tasks have no significant difference under the different conditions of r (Table 2). From the results of the TOSTs for r_τ, as shown in Table 2, the pair of r_τ under each condition of the perimeter ratio r in the double-ellipse task indicate a significant equivalence ($p < 0.03$). Also, the confidence intervals of the mean of the difference between $r_{\tau|r=1.5}$ and $r_{\tau|r=3.0}$ were contained within the interval $[-\delta, +\delta]$ in both significant levels 90% and 95% (Fig. 5). In the figure-eight task, all pairs of r_τ under each condition of the perimeter ratio r indicate no significant equivalence. The confidence intervals of the mean of the differences exceeded sufficiently for all pairs of r_τ (Fig. 5).

Next, we show the results of the statistical tests for r_d in Table 3 and Fig. 6. The results of r_d were quite different to that of r_τ. The results of the significant difference test, with two sample t-tests, for r_d show that all pairs of r_d, under each condition of r, indicate a significant difference without dependence on the trajectory shapes (Table 3). Furthermore, the result in the equivalence test of r_d with

Table 2
Result of the equivalence test of the DCTC ratio r_τ under each condition of the perimeter ratio r.

	Two sample t-test			Two one-sided t-test (TOST)			
	t_{diff} (28)	p_{diff}	Significance	t_L (28)	t_U (28)	max($[p_L, p_U]$)	Significance
Figure-eight							
$r_{\tau\|r=1.0}$ vs $r_{\tau\|r=2.0}$	−2.0788	0.0235	n.s. (FDR)	0.6963	−4.8538	0.2460	n.s. (FDR)
$r_{\tau\|r=1.0}$ vs $r_{\tau\|r=3.0}$	−2.1704	0.0193	n.s. (FDR)	−0.3409	−4.0000	0.6321	n.s. (FDR)
$r_{\tau\|r=2.0}$ vs $r_{\tau\|r=3.0}$	−0.7018	0.2443	n.s. (FDR)	0.9033	−2.3069	0.1870	n.s. (FDR)
Double-ellipse							
$r_{\tau\|r=1.5}$ vs $r_{\tau\|r=3.0}$	−0.0130	0.4949	n.s.	2.2959	−2.3219	0.0147	$p < 0.03$

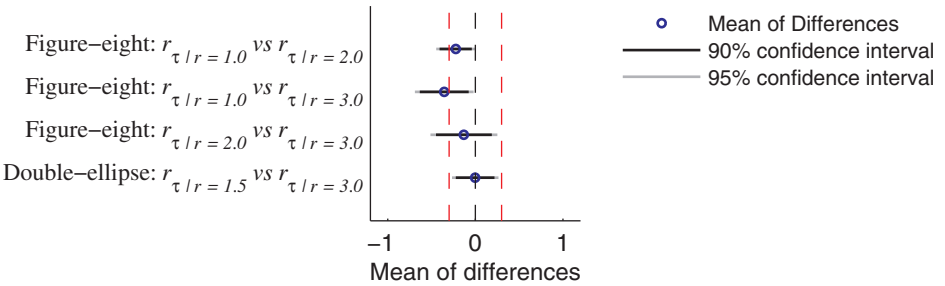

Fig. 5. Results of the equivalence test of the DCTC ratio r_τ under each pair of task conditions. The blue circular symbols indicate the mean of the differences between the different task conditions, $r_{\tau|r=n}$ indicates the DCTC ratio under the task condition of the perimeter ratio $r = n$. The black and gray bold lines show the 90% and 95% confidence intervals, respectively. The red broken lines represent the lower and upper equivalence boundaries $[-\delta, +\delta]$ (set as $\delta = 0.3$).

Table 3
Results of the equivalence test of the duration ratio r_d under each condition of the perimeter ratio r.

	Two sample t-test			Two one-sided t-test (TOST)			
	t_{diff} (28)	p_{diff}	Significance	t_L (28)	t_U (28)	max($[p_L, p_U]$)	Significance
Figure-eight							
$r_{d\|r=1.0}$ vs $r_{d\|r=2.0}$	−20.4382	1.1479×10^{-18}	$p < 0.01$ (FDR)	−9.8352	−31.0413	1.0000	n.s. (FDR)
$r_{d\|r=1.0}$ vs $r_{d\|r=3.0}$	−28.1839	2.1381×10^{-22}	$p < 0.01$ (FDR)	−19.8358	−36.5319	1.0000	n.s. (FDR)
$r_{d\|r=2.0}$ vs $r_{d\|r=3.0}$	−10.0053	4.7569×10^{-11}	$p < 0.01$ (FDR)	−3.0980	−16.9125	0.9978	n.s. (FDR)
Double-ellipse							
$r_{d\|r=1.5}$ vs $r_{d\|r=3.0}$	−11.5288	1.9050×10^{-12}	$p < 0.01$	−4.6142	−18.4434	1.0000	n.s.

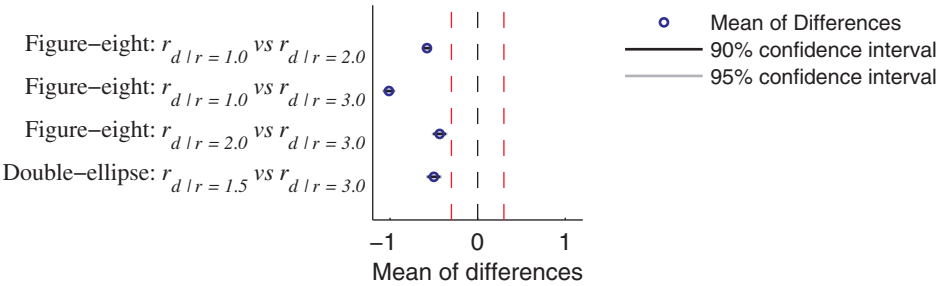

Fig. 6. Results of the equivalence test of the DCTC ratio r_d under each pair of task conditions. The blue circular symbols indicate the mean of the differences under the different task conditions, $r_{d|r=n}$ indicates the DCTC ratio under the task condition of the perimeter ratio $r = n$. The black and gray bold lines show the 90% and 95% confidence intervals, respectively. The red broken lines represent the lower and upper equivalence boundaries $[-\delta, +\delta]$ (set as $\delta = 0.3$).

TOSTs suggests no significance of equivalence for all pairs of r_d under each condition of r without dependence on the trajectory shapes (Table 3). As shown in Fig. 6, both the mean of the differences and the confidence intervals sufficiently exceeded the equivalence interval $[-\delta, +\delta]$ for all pair of r_d.

In summary, the movement time ratio r_d was not constant across different perimeter ratios. The DCTC ratio r_τ, in the result of the double-ellipse task, showed a value of around 1 and no significant difference across the different perimeter ratios. The result of the TOSTs further support the equivalence of the DCTC between the large and small loops for the double-ellipse task. However, the extent of equivalency of r_τ for the figure-eight task was not ensured statistically. These results suggest that human arm movement might be planned to maintain constant DCTCs between large and small loops, rather than a constant movement time. However, this tendency is dependent on the movement shape or task.

5. Discussion

Most previous studies on human motor control have not examined the computational relationship between trajectory planning and the isochrony phenomenon. Therefore, it remains unclear how the isochrony phenomenon is ensured during human arm movement tasks. In this study, we have considered the hypothesis that hand movement trajectory is generated to maintain a constant DCTC for large and small loops, rather than to maintain constant movement times (Wada & Kawato, 2004; Saito et al., 2006; Saito & Wada, 2006). To test this hypothesis, we defined the evaluation indexes r_d and r_τ, and calculated their values while forming two different shapes (a figure-eight and a double-ellipse). As a result, we suggested the possibility that human movement is planned to maintain constant DCTCs of large and small loops, rather than constant movement times. The feasibility of this computational theory has already been confirmed for the discrete and complex via-point movements in previous studies (Wada & Kawato, 2004; Saito et al., 2006; Saito & Wada, 2006). Thus, these results and the current results may provide evidence to support the applicability of the theory for both discrete and rhythmic movements. However, due to the fact that the tendency of a constant DCTC was not sufficiently supported in the results of the figure-eight task, there is the possibility that the tendency of a constant DCTC between the loops is conditionally supported, though this may be dependent on the trajectory shape or task. To consider our presented results and the limitations in this study, we discussed the relationship between the above-mentioned results and previous studies, as below.

5.1. General discussion of the human isochrony phenomenon

The isochrony phenomenon has been reported in many studies on the motor control of hand-reaching tasks (Viviani & McCollum, 1983; Sartori et al., 2013; Flash et al., 2013; Viviani & Terzuolo, 1982). These studies suggest that the behavioral tendency, through the speed of the reaching movement, is regulated to increase as its trajectory distance increases. Applying the same tasks as in our study, it has been reported that the ratio of the movement time between large and small loops is sufficiently smaller than the movement perimeter ratio, regardless of the movement size (Viviani & Flash, 1995). As shown in Fig. 4, our observed data for the movement time ratio is in agreement with this previous study (Viviani & Flash, 1995). Thus, we observed the same behavioral tendency as in the previous study.

Applying two types of t-test (two sample t-tests and TOSTs), we then evaluated how the DCTC ratio of large and small loops corresponds with the difference in the movement perimeter ratio r. If our measured data satisfy the condition shown in Fig. 1, the assumption that the hand movement trajectory acts to maintain constant DCTCs between large and small loops, rather than the isochrony phenomenon, is correct. As a result, the ratio of the DCTCs suggested the equivalence of r_τ under different conditions of r in the double-ellipse task, while the movement time ratio r_d indicated a significant difference and no equivalence for all pairs of r_d under the different conditions of r. Such results suggest that the constancy is more strongly reflected in the joint-torque changes than in the movement time (Table 2 and Fig. 5). This tendency, from the results of the double-ellipse task, is consistent with our hypothesis, as illustrated in Fig. 1.

However, as shown in Table 2, the results of the statistical tests for r_τ in the figure-eight task suggested a different tendency relative to the results of the double-ellipse task. A reason for this could be due to the differences in the joint-torque changes dependent on trajectory shape. From the results shown in Fig. 4A, the variance of the mean of r_τ appears to increase with the increase of the perimeter ratio r in the figure-eight task. The movement of the figure-eight task might be variable due to differences in strategy, or difficulty for each subject. To reveal this possibility, we considered the relationship between the movement time and torque change C_τ per one cycle in the figure-eight task. As an example of this consideration, we showed the results under the condition of the perimeter ratio $r = 3.0$ for the figure-eight task, shown in Fig. 7. The scatter plot in this figure indicates the trial-averaged value of each subject. Given this figure, the subject, who has the tendency to perform the task with a shorter movement time, had a larger score of C_τ per one cycle during reaching in the figure-eight task. Moreover, the variance of C_τ drastically increased relative to the decrease in the average movement time per cycle. We believe that such a difference of C_τ, depending on the movement time, might affect the tendency for constancy of the DCTC ratio during a reaching task. Furthermore, as shown in Fig. 7, while both the mean value and variance of C_τ drastically changes depending on the movement time in the range of less than around 1.5 s, the values of C_τ converge around certain amplitudes in the range of a movement time over 1.5 s. This indicates the possible domain of the movement speed to satisfy the constancy of the DCTC ratio during a reaching task.

As for other reasons to explain the different tendencies between the double-ellipse and figure-eight tasks, we should consider how the differences in the movement direction between the small and large loops affect the tendency of constant DCTCs during reaching. Whereas the movement direction is the same for both the loops in the double-ellipse task, the movement direction is different for the loops in the figure-eight task. Thus, the figure-eight task seems to be more complex than the double-ellipse task. The changing

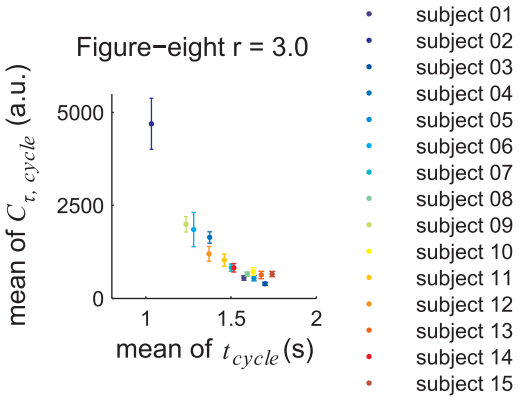

Fig. 7. Relationship between the movement time and torque changes per cycle (Figure-eight task, $r = 3.0$). The value of the x-axis indicates the within-subject average of the movement time per cycle. The value of the y-axis indicates the within-subject average of the objective function C_τ per cycle. The scatter plot indicates the value for each subject. The error bars indicate the inter-trial standard deviation of the C_τ per cycle for each subject.

direction between loops could result in different temporal changes of muscle recruitment for both the shoulder and the elbow. Such changes could affect DCTCs.

However, to clarify the above possible reasons, further consideration is required with additional experiments and analyses for future work, because there is a lack of experimental evidence for both the effects of the movement direction and variance, depending on the trajectory shapes, for the mechanism of joint-torque changes during hand movement. Thus, these additional requirements constitute the limitation of this study to generalize our hypothesis.

5.2. Relationship with other conventional studies

In this paper, we have presented experimental evidence to confirm that the isochrony phenomenon is a result of optimizing the movement time based on the minimum commanded torque change criterion. Compared with previous studies on trajectory planning (Viviani & McCollum, 1983; Flash & Hogan, 1985; Sartori et al., 2013; Flash et al., 2013; Viviani & Terzuolo, 1982), the advantage of our study is that we have demonstrated the relationship between the isochrony principle and human arm dynamics (e.g. torque changes) during the reaching task.

Relevant computational studies have reported two typical findings based on the minimum jerk criterion. First, previous studies (Viviani & Terzuolo, 1982; Bennequin, Fuchs, Berthoz, & Flash, 2009; Flash et al., 2013) have suggested geometrical reasons for the isochrony principle of hand movement organization. In these studies, from the point of view of the geometric relationship between the certain planar movement path r and the affine-transformed path $\bar{r}$, the authors found the movement time to be independent of the difference in movement size between r and $\bar{r}$ (i.e., the isochrony principle). For the second, we could consider the findings suggested by Huh and Sejnowski (2015) that the one-third power law for curved hand movements could be mathematically explained based on the framework of the minimum jerk criterion. This finding may explain the mathematical relationship between movement curvature and movement speed during curved hand movement tasks.

These findings are based on a similar concept as our study, as the author attempted to explain a specific phenomenon during human hand movement tasks based on the computational criterion of trajectory planning. However, these typical findings from the above are based on the minimum jerk criterion, and this criterion is on the basis of the hypothesis where the CNS first plans the desired trajectory at the task-oriented coordinates (such as the visual coordinate system) during the hand reaching task (Edelman & Flash, 1987; Kyriakopoulos & Saridis, 1988; Uno et al., 1989; Flash & Hogan, 1985). Therefore, even though the minimum jerk criterion can generate a simulated trajectory which indicates a similar path relative to the trajectory drawn by the hand, the determined trajectory using this criterion is independent of dynamic property, such as the joint-torque. Thus, the above-mentioned findings do not directly describe the relationship with the effect of the human arm dynamics in such situations as when the measured trajectory of human arm movement is consistent with the isochrony phenomenon. Moreover, in order to reveal the relationship between the aforementioned previous findings (Viviani & Terzuolo, 1982; Bennequin et al., 2009; Flash et al., 2013; Huh & Sejnowski, 2015) and our presented findings, further study is required with additional considerations. For example, we should attempt to explain the effect of DCTCs in the situation as when the geometric relationship between the certain planar movement path r and the affine-transformed path $\bar{r}$ is satisfied during hand movement tasks.

In addition, we should note that one limitation of our study is the total movement time. Previously, a study of the computational theory of human arm movement with single-joint reaching suggested the possible relationship between trajectory planning and movement time (Tanaka, Krakauer, & Qian, 2006). The authors of this study (Tanaka et al., 2006) suggested a computational model that could predict the entire movement time. However, in our study, we did not estimate the total movement time while estimating the via-points and duration between them. As the model suggested by Tanaka et al. (2006) considers only the entire movement time for single-joint reaching, it may not be easy to incorporate their model into ours currently. This is necessary to examine in future

works.

6. Conclusion

In summary, we have presented experimental evidence that human hand movement is optimized to satisfy the tendency whereby the DCTCs are statistically equivalent for large and small loops during a double-ellipse task. This evidence is partially consistent with our hypothesis (Saito et al., 2006; Saito & Wada, 2006). Further, these facts implicitly indicate the possibility that the isochrony phenomenon is observed as a secondary effect of the computational process to ensure above condition during hand reaching tasks. Even though many previous studies have found experimental evidence to suggest the existence of the isochrony phenomenon during human reaching tasks, these findings have not provided a sufficient explanation for the computational relationship between trajectory planning and the isochrony phenomenon. Therefore, our results have implications for how this phenomenon is ensured through the motor control of human arm movements via the computational criterion of trajectory planning.

However, as discussed above, the tendency toward constant DCTCs between loops still faces the issue of differing depending on the shape of trajectory and movement direction. To explore this issue, further consideration is required with additional experiments and analyses. Moreover, our results do not explain the relationship between neural activity and the commanded torque changes criterion. These limitations of the present study represent important topics for future work.

Acknowledgments

This research was partially supported by the JSPS KAKENHI (24300051, 26560303, 15K12597). We thank Stuart Jenkinson, PhD, from Edanz Group (www.edanzediting.com/ac) for editing a draft of this manuscript.

References

Benjamini, Y., & Hochberg, Y. (1995). Controlling the false discovery rate: A practical and powerful approach to multiple testing. *Journal of the Royal Statistical Society, 57*, 289–300. https://doi.org/10.2307/2346101. arXiv:95/57289.

Bennequin, D., Fuchs, R., Berthoz, A., & Flash, T. (2009). Movement timing and invariance arise from several geometries. *PLoS Computational Biology, 5*, e1000426.

Dornay, M., Kawato, M., & Suzuki, R. (1996). Minimum Muscle-Tension Change Trajectories Predicted by Using a 17-Muscle Model of the Monkey's Arm. *Journal of Motor Behavior, 28*, 83–100. https://doi.org/10.1080/00222895.1996.9941736.

Edelman, S., & Flash, T. (1987). A model of handwriting. *Biological Cybernetics, 57*, 25–36.

Flash, T., & Hogan, N. (1985). The coordination of arm movements: an experimentally confirmed mathematical model. *The Journal of Neuroscience, 5*(1688–1703), 4020415.

Flash, T., Meirovitch, Y., & Barliya, A. (2013). Models of human movement: Trajectory planning and inverse kinematics studies. *Robotics and Autonomous Systems, 61*, 330–339. https://doi.org/10.1016/j.robot.2012.09.020.

Gomi, H., & Osu, R. (1998). Task-dependent viscoelasticity of human multijoint arm and its spatial characteristics for interaction with environments. *Journal of Neuroscience, 18*, 8965–8978.

Huh, D., & Sejnowski, T. J. (2015). Spectrum of power laws for curved hand movements. *PNAS, I*, 201510208. https://doi.org/10.1073/pnas.1510208112.

Kawato, M., Maeda, Y., Uno, Y., & Suzuki, R. (1990). Trajectory formation of arm movement by cascade neural network model based on minimum torque-change criterion. *Biological Cybernetics, 62*, 275–288.

Kudo, N., Choi, K., Kagawa, T., & Uno, Y. (2016). Whole-body reaching movements formulated by minimum muscle-tension change criterion. *Neural Computation, 28*(5), 950–969.

Kyriakopoulos, K. J., & Saridis, G. N. (1988). Minimum jerk path generation. IEEE.

Lakens, D. (2017). Equivalence Tests: A Practical Primer for t Tests, Correlations, and Meta-Analyses. *Social Psychological and Personality Science, 8*, 355–362 arXiv:1948550617697177.

Nakano, E., Imamizu, H., Osu, R., Uno, Y., Gomi, H., Yoshioka, T., & Kawato, M. (1999). Quantitative examinations of internal representations for arm trajectory planning: minimum commanded torque change model. *Journal of Neurophysiology, 81*, 2140–2155.

Saito, H., Tsubone, T., & Wada, Y. (2006). Can human isochrony be explained by a computational theory? Annual International Conference of the IEEE Engineering in Medicine and Biology – Proceedings, (pp. 4494–4497). DOI: 10.1109/IEMBS.2006.260819.

Saito, H., & Wada, Y. (2006). Movement time planning between via-points in human movement. Annual International Conference of the IEEE Engineering in Medicine and Biology – Proceedings, (pp. 1208–1211).

Sartori, L., Camperio-Ciani, A., Bulgheroni, M., & Castiello, U. (2013). Reach-to-grasp movements in macaca fascicularis monkeys: The isochrony principle at work. *Frontiers in Psychology, 4*, 1–5. https://doi.org/10.3389/fpsyg.2013.00114.

Tanaka, H., Krakauer, J. W., & Qian, N. (2006). An optimization principle for determining movement duration. *Journal of Neurophysiology, 95*, 3875–3886. https://doi.org/10.1152/jn.00751.2005.

Uno, Y., Kawato, M., & Suzuki, R. (1989). Formation and control of optimal trajectory in human multijoint arm movement. *Biological Cybernetics, 61*, 89–101.

Viviani, P., & Flash, T. (1995). Minimum-jerk, two-thirds power law, and isochrony: converging approaches to movement planning. Journal of experimental psychology. *Human Perception and Performance, 21*, 32–53. https://doi.org/10.1037/0096-1523.21.1.32.

Viviani, P., & McCollum, G. (1983). The relation between linear extent and velocity in drawing movements. *Neuroscience, 10*, 211–218. https://doi.org/10.1016/0306-4522(83)90094-5.

Viviani, P., & Terzuolo, C. (1982). Trajectory determines movement dynamics. *Neuroscience, 7*, 431–437.

Wada, Y., Kaneko, Y., Nakano, E., Osu, R., & Kawato, M. (2001). Quantitative examinations for multi joint arm trajectory planning?using a robust calculation algorithm of the minimum commanded torque change trajectory. *Neural Networks, 14*, 381–393.

Wada, Y., & Kawato, M. (1993). A neural network model for arm trajectory formation using forward and inverse dynamics models. *Neural Networks, 6*, 919–932. https://doi.org/10.1016/S0893-6080(09)80003-8.

Wada, Y., & Kawato, M. (2004). A via-point time optimization algorithm for complex sequential trajectory formation. *Neural Networks, 17*, 353–364. https://doi.org/10.1016/j.neunet.2003.11.009.